

**NASA Technical Memorandum 79178**

**(NASA-TM-79178) AN EXPERIMENTAL, LOW-COST,  
SILICON SLURRY/ALUMINIDE HIGH-TEMPERATURE  
COATING FOR SUPERALLOYS (NASA) 24 p  
HC A02/MF A01**

**N79-29292**

**CSCL 11P**

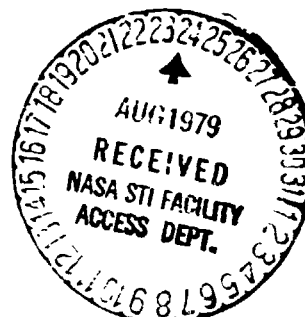
**Unclas  
31689**

**G3/26**

**AN EXPERIMENTAL, LOW-COST, SILICON  
SLURRY/ALUMINIDE HIGH-TEMPERATURE  
COATING FOR SUPERALLOYS**

**Stanley G. Young and Daniel L. Deadmore  
Lewis Research Center  
Cleveland, Ohio**

**July 1979**



## SUMMARY

A potentially low-cost coating has been developed that exhibits significant protection of superalloys from high-temperature, high-gas-velocity oxidation, thermal fatigue, and hot corrosion. The coating was formed by applying a slurry-spray of high-purity silicon followed by a 16-hour, 1100° C pack aluminizing treatment. NASA VIA and B-1900 nickel-base, turbine-blade superalloys were the substrate materials.

When cyclically tested in Mach 1 combustion gases, the Si-Al coating on alloy VIA protected the base metal from oxidation about four times longer than conventional aluminides and from thermal fatigue to about the same level. More expensive Pt-Al coatings or MCrAlY (where M is Ni and/or Co) coatings, deposited by the physical vapor deposition (PVD) process, are the only ones observed to last longer or provide equal protection to VIA. On alloy B-1900 the Si-Al coating exceeded the performance of a Pt-Al coating on VIA in both oxidation and thermal fatigue. Also, the Si-Al coating significantly increased the resistance of B-1900 to hot corrosion.

Studies of the failure processes indicated that for oxidation a small pit, fissure, or blister of the coating at either the test specimen leading or trailing edge appeared to lead to a thermal fatigue crack, which propagated and provided an expanded area for oxidation. For hot corrosion, the failure process was started by a blister that formed in the coating and allowed very rapid corrosion of the substrate from that site.

Preliminary microstructural, X-ray, and electron microprobe studies were made before and after testing. It is believed that the silicon in the coating contributed to the formation of SiO<sub>2</sub> in the protective Al<sub>2</sub>O<sub>3</sub>. The presence of the substrate elements Ta and Mo, also detected in the complex protective oxide scale, indicated that they had diffused from the substrate to the protective scale.

## INTRODUCTION

The efficiency of gas-turbine engines increases as the operating temperatures increase. Such operating temperatures, however, are now restricted by design limitations, by material strength deterioration, and by material capability to resist oxidation and hot-corrosion attack. For metal temperatures above 900° C, nickel- and cobalt-base superalloy components usually must be coated to resist such attack. At the Lewis Research Center there has been a continuing effort to improve conventional aluminide coatings and to develop new, alternative coatings such as claddings, physical vapor deposited (PVD) MCrAlYs, aluminized NiCrAlSi, and Pt-Al systems (refs. 1 to 5). The primary advantage of these systems is that they form an adherent Al<sub>2</sub>O<sub>3</sub> film which protects the substrate from further oxidation.

Refractory metals and alloys developed for much higher temperatures than superalloys can be protected by fused-silicide coatings (refs. 6 and 7). These

alloys are generally protected by  $M_5Si_3$  and  $MSi_2$  silicide compounds, which primarily form  $SiO_2$  upon oxidation (ref. 8). Little is known, however, about the oxidation of Ni-Si and Co-Si alloys as coatings compared with the MAI and MCrAlY coating alloys. Even less is known about the complex combinations of oxides, intermetallic compounds, and eutectics that could result from silicide/aluminide and  $SiO_2/Al_2O_3$  combined with the nine or more other elements contained in many superalloys.

Most available information indicates that small amounts of silicon have a favorable effect on the oxidation resistance of iron and nickel-base alloys (refs 9 to 12). Some researchers, however, have reported unfavorable effects (ref. 13), and another researcher reported both good and bad effects, depending on the substrate alloy (ref. 8). It appears that silicon in a coating must be tailored for use with the particular substrate to insure its beneficial effects.

The study by Smialek (ref. 8) of fused silicide coatings on superalloys tested in 1-hour cyclic furnace oxidation tests clearly indicated that further study of silicon-rich coatings was warranted. Other unpublished cyclic furnace oxidation data (by D. Deadmore of Lewis) showed that a 100 percent silicon-slurry spray followed by a standard pack aluminizing treatment greatly improved the high-temperature oxidation resistance of NASA VIA alloy.

The purpose of this investigation was to evaluate the potential of the Si-Al coating system in more severe environments that more closely simulate those of gas-turbine engines and to compare these results with previously tested or baseline (in service) coating systems. If the Si-Al coating system could be shown to approach or exceed the protection afforded by these other systems, a large potential would exist for coating cost reduction.

Specimens of the nickel-base alloys NASA VIA and B-1900 were slurry-spray coated with 100 percent silicon and subjected to an aluminide pack treatment. These as well as uncoated specimens were evaluated for oxidation and thermal fatigue in Mach 1 burner tests under cyclic conditions from room temperature to about 1093° C. In addition, the B-1900 specimens were also tested at 900° C with 5 ppm synthetic sea salt injected into the hot-gas stream of a Mach 0.3 burner to evaluate hot-corrosion resistance. The coated and uncoated materials' environmental resistances were judged on the basis of weight change, thermal fatigue cracking, and various post-test microstructural examinations.

## MATERIALS, APPARATUS, AND PROCEDURES

### Materials and Specimen Preparation

The nominal compositions of the substrate alloys (in wt %) are for VIA, nickel - 6 chromium - 7 cobalt - 5 aluminum - 2 molybdenum - 1 titanium - 6 tungsten - 9 tantalum - 0.5 hafnium - 0.5 niobium - 0.4 rhenium; and for B-1900, nickel - 8 chromium - 10 cobalt - 6 aluminum - 6 molybdenum - 1 titanium - <0.1 tungsten - 4 tantalum - 0.1 carbon - 0.1 zirconium - 0.015 boron.

The two specimen configurations used in this investigation are shown in figure 1 (from ref. 14). The oxidation and thermal fatigue specimen was 10.6 by 2.54 by 0.63 cm and was tapered along one long edge with a 45° included angle and an 0.8-mm radius. The hot-corrosion specimen was basically a 1.27-cm-diameter round with two flats along the length at an included angle of 30°.

Specimens were cleaned in a wet-slurry grit-blast facility. They were then ultrasonically cleaned in alcohol and then acetone. The coating was applied to the test specimens in the following manner: a lacquer slurry containing 4 grams of high purity silicon powder per 10 ml of vehicle was air-brushed (sprayed) onto the superalloy specimens to a specific weight of 6 mg Si/cm<sup>2</sup>. The sprayed specimens were then air dried for 24 hours. The silicon was 99.9 percent pure and was of a nominal powder size of -325 mesh. The lacquer was a cellulose nitrate solution that served as both the transport vehicle and binder.

After they were dry, the specimens were placed in a pack of 98 percent Al<sub>2</sub>O<sub>3</sub>, 1 percent NaCl, and 1 percent Al powder. The pack was heated to 1100° C for 16 hours under argon. Weight pickup in the pack averaged 17 mg/cm<sup>2</sup>. The pack was then removed from the furnace and allowed to cool for 4 hr to room temperature before specimens were removed from the pack. With each pack, a small test coupon of the same material was coated so metallurgical examination of the as-coated material could be performed without destroying a burner rig specimen.

### High-Gas-Velocity Test Apparatus

Oxidation and thermal fatigue specimens were run in a natural-gas fueled burner rig operating with a gas velocity at the burner nozzle of Mach 1. A detailed description of the burner facility and conditions can be found in references 15 and 16. An overall view and a schematic diagram of the facility are shown in figure 2. In each test cycle the specimens were rotated in the air-rich natural gas combustion products for 1 hour at a metal temperature of 1093° C. The specimen holder assembly is shown in figure 3(a). The 45° tapered edges of the specimens were closest to the nozzle. At the end of each hour the specimens were lowered into a high-velocity (approx. Mach 1) cooling air blast for 3 min, which rapidly cooled the specimens to room temperature.

The hot-corrosion specimens were run in a similar but smaller, facility operating on Jet A fuel with a gas velocity of Mach 0.3. Five ppm of synthetic sea salt was added to the combustion gases. The specimens were rotated in the gas flame for 1 hr at 900° C and then cooled to near room temperature in 3 min. A photograph of the hot-corrosion specimen holder is shown in figure 3(b).

In both the oxidation and thermal fatigue test and the hot-corrosion test temperatures were calibrated using slip-ring and thermocouple arrangements connected to dummy specimens in the rotating specimen holder assembly, and were controlled by a stationary control thermocouple downstream of the test specimens. Temperature checks were also made with a calibrated optical pyrometer. Specimen temperature was maintained at ±8° C from the operating temperature.

## Test Procedure and Post-Test Analysis

Before testing, the specimens were degreased in trichlorethylene vapor and weighed to the nearest 0.1 milligram. At intervals of either 20 or 50 hr of testing, the specimens were removed from the apparatus, reweighed, photographed, and inspected for cracks. Each test was run with two uncoated specimens and two specimens with the coating.

After burner tests were complete, as determined from the appearance of the specimen or weight loss rate (observation of severe cracking or erosion), the specimens were cut into sections and mounted for metallographic inspection. Some samples of surface oxides were scraped from the tapered edges of the oxidation and thermal fatigue specimens for X-ray diffraction analyses. Microprobe analysis was conducted on the coated VIA specimens before and after exposure to determine the extent of diffusion of silicon into the alloy and to indicate elements present in the metallic and oxide forms.

## OXIDATION AND THERMAL FATIGUE

### Weight-Change Results

The results of the 1093° C, cyclic, Mach 1 burner-rig tests on coated and uncoated alloy specimens are shown in figure 4. In these figures the curves drawn through actual points are for the Si-Al coating data, which were gathered in the current series of tests. The other curves are data from tests performed by other researchers in the same burner facility, under the same conditions. They are included here for comparison.

Figure 5 (from ref. 1) is a schematic diagram of a typical weight-change curve for high-gas-velocity burner-rig testing. Several parameters shown in this diagram can be used to compare the ability of the various systems to withstand the tests (i.e., oxidation resistance, time to thermal fatigue cracking, and hot-corrosion resistance). The parameter  $t_1$  is the time in hours (and, therefore, number of cycles) to the point of maximum weight gain;  $t_2$  is the time to the point where the weight-change curve crosses the zero axis. At this point the specimen is usually losing weight at an increasing rate and is deteriorating rapidly. Specimens were removed from the test after a weight change of -50 mg or if a thermal-fatigue crack had propagated approximately 1/3 of the way through the specimen, increasing the danger of burner bar fracture. The point on the weight-change curve where a thermal-fatigue crack is first noted is designated either LEC (leading edge crack) or TEC (trailing edge crack).

In figure 4 large spreads are noted between the weight-change curves of supposedly identical specimens. Such scatter is very common, however, in this type of test due to the many uncontrollable parameters in the coating application process. Automated spray or electrophoretic deposition systems may result in much better reproducibility.

From figure 4(a), the Si-Al coated specimens have lives (as measured by  $t_2$ ) of from 675 to 960 hr. That is nearly 4 times the life of commercial pack-aluminide specimens tested under the same conditions. The uncoated specimen shows rapid weight loss. The Pt-Al specimen (from ref. 1) had an extrapolated life approximately twice that of the Si-Al coated VIA specimen. The curve for this specimen is shown in both figures 4(a) and (b).

When the Si-Al coating was applied to B-1900 (which had a shorter life with an aluminide coating than aluminide coated VIA from ref. 1), a burner rig life of one of the specimens ( $t_2$  of 1500 hr) even surpassed the reported data for the Pt-Al on VIA system by 100 hr. The Si-Al coated B-1900 specimen was actually run to 2100 hr in the burner rig before removal. No thermal fatigue cracks were observed until after 800 hr (200 hr longer than that reported for the Pt-Al specimen). These tests clearly demonstrated the potential of the Si-Al coating when applied to those alloys that form favorable combinations with this protective coating.

Most of the preceding data are summarized in the bar-chart of figure 6. Also comparisons are made with several other coatings evaluated in reference 1. From this figure it can be seen that the Si-Al coatings on VIA protected the base metal from oxidation approximately 4 times longer than conventional aluminides. Thermal fatigue protection was about equal to slightly better than commercial aluminides. The Pt-Al coating had a longer oxidation life; however, the curve for this material was extrapolated to 1400 hr. A physical-vapor-deposited CoCrAlY coating on VIA also exhibited approximately equal or slightly better oxidation resistance with an extrapolated value of 1000 hr for  $t_2$ . One of the specimens, Si-Al coatings on B-1900, slightly exceeded the performance of the Pt-Al coating on NASA VLA (>1500 hr) and significantly out-performed all the other coatings of reference 1 in oxidation and thermal fatigue resistance.

### Photographic Results

Photomicrographs were taken of the Si-Al coated specimens at various stages of the oxidation tests (figs. 7 and 8). All of these photographs are side views of the burner bar at approximately actual size with the tapered leading edges facing to right. Each figure shows the two specimens used with each substrate material. The VIA alloy specimens are shown in figure 7 and the B-1900 alloy specimens are shown in figure 8.

Specimen 1 (fig. 7(a)) showed a small white spot near the leading edge at 126 hr which showed up as a pit in the 217-hr photograph. After 337 hr a microcrack was observed which continued to propagate and widen until the end of the test. Specimen 2 (fig. 7(b)) showed a pit at 427 hr and several others at 627 and 727 hr. A crack can be seen (at the site of the original pit) at 822 hr. By 922 hr this crack had lengthened and some peeling of the coating has occurred. Specimen 2 was clearly superior in its endurance, so the weight loss due to oxidation of the cracked area of specimen 1 appears to be far more significant than that associated with coating loss observed on specimen 2.

For the B-1900 substrate, specimen 1 (fig. 8(a)) ran the longest time (2129 hr) and, even though it was cracked and had lost >200 mg, it looked remarkably good. A very fine fissure was observed on the trailing edge after 800 hr and this continued to grow throughout the test. Several other cracks appeared later, in both the leading and trailing edges. Specimen 2 (fig. 8(b)) showed a small TEC after 600 hr. Also the coating appeared to deteriorate over a larger area of the leading edge at the same time. Further cracking and some erosion of the specimen was observed (note the macrophotograph of the specimen at 1650 hr). Specimen 1 did not show as much erosion even though it ran nearly 500 hr longer. Again, this scatter points out the need for automated coating techniques or better control of the coating process to obtain greater reproducibility.

### Metallography and Analysis

Test coupons of the as-coated specimens and cross sections of the as-tested specimens were cut and mounted in standard metallographic mounts. Photomicrographs are shown in figures 9 to 12. Figure 9 shows the Si-Al on VIA alloy as coated; figure 10 shows the same alloy and coating after testing in the Mach 1 burner rig for more than 1000 hr at 1093° C. Figure 11 shows the coating on B-1900 alloy, and figure 12 shows the coated B-1900 system after 2000 hr of cyclic testing.

An electron microprobe X-ray analysis (EMXA) was made of the VIA specimen before and after the cyclic exposure (fig. 13). Information gained from this EMXA study was used to aid in the understanding of phases observed in figures 9 and 10.

Returning to the as-coated VIA specimen of figure 9, two distinct layers were observed above the VIA substrate. The inner layer is what remains of the original silicon-sprayed layer after the 16-hr pack treatment. This layer appeared as a multiphase, multielement region of small elongated grains. This layer was highest in nickel, then silicon, with widely varying amounts of the other elements. One interesting aspect of this study was that silicon diffusion into the base metal was very slight (much less than expected) but that silicon diffusion outward was significant. The top layer was mostly NiAl, which contained nodules of the silicon-rich phase and, as a result, formed an unusual pebb'y textured surface. These nodules may have been the result of silicon particle agglomeration in the spray process. However, the surface appeared to be covered relatively uniformly with these rounded grains that had an estimated average diameter of about 100  $\mu$ m. After exposure, this surface tended to become smoother, yet, this pebb'y texture remained long into the tests.

After the 1000-hour burner rig exposure, the coating appeared entirely different (see fig. 10). Layers were not as distinct, and larger grains of discontinuous phases were present. Even the base metal had been affected by the thermal exposure, and larger phases were observed in the matrix. Silicon dif-

fused about 200  $\mu\text{m}$  deeper into the substrate. Two distinct phases were observed in the originally silicon-rich zones close to the substrate. The continuous phase is rich in aluminum, nickel, and cobalt, and the dispersed darker phase is rich in silicon, titanium, tungsten, chromium, molybdenum, and tantalum. Above this region a large-grained phase, rich in chromium, silicon, nickel, aluminum, and cobalt and containing numerous twins, was observed. This phase may be a form of low-aluminum martensitic  $\beta$ -NiAl as described in reference 8. At the surface small portions of a metallic phase rich in nickel, aluminum, tantalum, tungsten, and titanium (light region) were present. This is believed to be either nickel solid solution or  $\text{Ni}_3\text{Al}$ . In the oxides, molybdenum, tantalum, silicon, and aluminum were detected. X-ray analysis of material scraped from the surface picked up  $\text{Al}_2\text{O}_3$ ,  $\text{SiO}_2$ , nickel solid solution, spinel, and a number of other possible or unidentified phases.

It appears that the high silicon phases combine with tantalum and molybdenum from the substrate and that these elements diffuse rapidly into the outer nickel- and aluminum-rich phases in sufficient quantities to allow other protective oxides, in addition to  $\text{Al}_2\text{O}_3$ , to form. If this is the case, the protective ability of this coating would be highly sensitive to the elements contained in the substrate. Small amounts of silicon in the alloy have been shown to increase the oxidation resistance of B-1900 (ref. 17) and  $\text{Ni}_3\text{Al}$  (ref. 18). Further analysis is needed to more clearly identify specific phases, but the complexity and high number of elements makes this very difficult.

The as-coated test coupon of the Si-Al coating on B-1900 in figure 11 shows features similar to the coating on VIA. After testing (fig. 12) the surface appeared even less stratified than on the VIA specimen. Although not shown here, scattered grains of a twinned phase were also observed. The longer test (2000 instead of 1000 hr) may account for some differences. X-ray analysis of material scraped from the surface included  $\text{Al}_2\text{O}_3$ , nickel solid solution, spinel, and other unidentified phases. Additional analysis is also needed to characterize this coating more completely.

## HOT-CORROSION RESULTS

The results of the hot-corrosion tests on bare and Si-Al coated B-1900 are shown in figure 14. Two specimens of each system were subjected to an accelerated test involving exposure to Mach 0.3 combustion gases containing 5 ppm sea salt and were cycled between 900° C and room temperature. From the figure it is obvious that the coating protects B-1900 in that the weight change did not become negative until after 500 hours as compared to less than 50 hours for the uncoated specimens.

Figure 15 shows the appearance of the bare specimens after 105 hours of test and illustrates the severity of the hot corrosion process to this alloy. Figure 16 shows the coated specimens at various times to the end of the test. Note that blisters formed after 345 hr. Hot corrosion occurred at these spots and essen-



tially made deep holes in the specimens by 779 hours. Although the long-time specimens appear bad from the photographs, the coating actually provided relatively good resistance for such a severe type of test.

## CONCLUSIONS

High-gas-velocity burner rig tests were conducted to evaluate the relative oxidation resistance, thermal fatigue resistance, and hot-corrosion resistance of a new duplex silicon-aluminide coating on two nickel-base superalloys. The results were compared with published data on other conventional and advanced coatings. This work was conducted with the objective of finding a low-cost coating for protecting hot-section components of gas-turbine engines. The coating consisted of a slurry-sprayed layer of high-purity silicon followed with a 16-hour, 1100° C pack aluminide process. NASA VIA and B-1900 nickel-base superalloys were the substrates. The following results were obtained:

(1) In Mach 1, 1093° C cyclic oxidation and thermal fatigue tests, the Si-Al coatings protected the VIA alloy at least four times longer than conventional aluminide coatings and provided about the same thermal fatigue protection. The more expensive Pt-Al and physical-vapor-deposited MCrAlY coating systems have shown approximately the same or greater resistance under the same test conditions.

(2) One of the Si-Al on B-1900 specimens slightly exceeded the oxidation and thermal fatigue performance of the Pt-Al coating on NASA VIA (ref. 1) and significantly surpassed PVD CoCrAlY on VIA in oxidation and thermal fatigue.

(3) The Si-Al greatly improved B-1900's resistance to hot corrosion in 5 ppm salt at Mach 0.3 at 900° C (500 hr compared to 50 hr uncoated).

(4) The Si-Al coating failure process in these oxidation tests started at either a pit, a fine fissure, or a small blister in the coating (at either the leading or trailing edge). This was followed by a thermal fatigue crack at that spot, which then propagated and allowed an expanded area of base metal to be exposed to oxidation.

(5) The Si-Al failure process in hot-corrosion tests started with a blister or pit which formed in the coating exposing the base metal. Rapid corrosion and oxidation of the base metal masked any other effects.

(6) Preliminary microstructural, X-ray, and electron microprobe studies after oxidation tests indicated that the high silicon phase, which also contained high amounts of tantalum and molybdenum from the substrate, supplied a combination of these elements to the original NiAl and/or nickel solid solution at the surface to allow combinations of oxides of silicon, tantalum, and molybdenum to form in addition to  $\text{Al}_2\text{O}_3$ . The protective ability of this coating appears to be highly sensitive to the elements contained in the substrate.

## REFERENCES

1. Deadmore, Daniel L.: High Velocity-Oxidation Performance of Metal-Chromium-Aluminum (MCrAl), Cermet, and Modified Aluminide Coatings on IN-100 and Type VIA alloys at 1093° C. NASA TN D-7530, 1974.
2. Talboom, F. P.; Elam, R. C.; and Wilson, L. W.: Evaluation of Advanced Superalloy Protection Systems. (PWA-4055, Pratt & Whitney Aircraft, NASA Contract NAS3-12415.) NASA CR-72813, 1970.
3. Levine, Stanley R.: Cyclic Furnace and High-Velocity Oxidation of an Aluminide-Coated High Strength Nickel Alloy (B-1900). NASA TM X-2370, 1971.
4. Gedwill, M. A.; and Grisaffe, S. J.: Oxidation Resistant Claddings for Superalloys. Met. Eng. Q., vol. 12, May 1972, pp. 55-61.
5. Freche, John C.; and Ault, G. Mervin: Progress in Advanced High Temperature Materials and Coating Technology. NASA TM X-73628, 1977.
6. Priceman, Seymour; and Kubick, Richard: Development of Protective Coatings for Columbium Alloy Gas Turbine Blades. Final Tech. Rep. 1 July 1969-30 July 1971, Sylvania Electric Products, Inc., June 1972, p. 33, (AFML-TR-71-172, AD-748837.)
7. Packer, C. M.; and Perkins, R. A.: Modified Fused Silicide Coatings for Tantalum (Ta-10W) Reentry Heat Shields. (D316824, Lockheed Missiles and Space Co.; NASA Contract NAS3-14316.) NASA CR-120877, 1973.
8. Smialek, James L.: Fused Silicon-Rich Coatings for Superalloys. NASA TM X-3001, 1974.
9. Zemskov, G. V.; et. al.: Effect of Silicon Additions on the Oxidation Resistance of Aluminided Layers on a Nickel-Chromium Alloy. Zashchitnye Pokrytiia na Metallakh, No. 4, 1971, pp. 151-158. Protective Coatings on Metals. Vol. 4, G. V. Samsonov, ed. (Z. S. Michalewicz, transl.) Consultant Bureau, 1972, pp. 110-113.
10. Moore, V. S.; Brentnall, W. D.; and Stetson, A. R.: Evaluation of Coatings for Cobalt- and Nickel-Base Superalloys, Vol. 2, Aluminide Protective Coatings For Nickel and Cobalt Alloys. (RDR-1474-3, Solar; NASA Contract NAS3-9401.) NASA CR-72714, 1970.
11. Crouch, A. G.; and Dooley, R. B.: The Mechanical Integrity and Protective Performance of Silica Coatings. Corros. Sci., vol. 16, no. 6, June 1976, pp. 341-347.
12. Lavendel, H. W.: Corrosion-Resistant Aluminide Coatings for Iron- and Nickel-Base Alloys. J. Metals, vol. 27, July 1965, pp. 4-10.

13. Fiedler, H. C.; and Sieraski, R. J.: Aluminide Coatings for Nickel-Base Alloys. (SRD-72-028, General Electric Co.; NASA Contract NAS3-14300.) NASA CR-120871, 1971.
14. Johnston, James R.; and Young, Stanley G.: Oxidation and Thermal Fatigue of Coated and Uncoated NX-188 Nickel-Base Alloy in a High-Velocity Gas Stream. NASA TN D-6795, 1972.
15. Deadmore, Daniel L.: Cyclic Oxidation of Cobalt-Chromium-Aluminum-Yttrium and Aluminide Coatings on IN-100 and VIA Alloys in High Velocity Gases. NASA TN D-6842, 1972.
16. Johnston, James R.; and Ashbrook, Richard L.: Oxidation and Thermal Fatigue Cracking of Nickel- and Cobalt-Base Alloys in a High-Velocity Gas Stream. NASA TN D-5376, 1969.
17. Miner, Robert V., Jr.; and Lowell, Carl E.: Effects of Silicon Additions on Oxidation and Mechanical Behavior of the Nickel-Base Superalloy B-1900. NASA TN D-7989, 1975.
18. Lowell, Carl E.; and Santoro, Gilbert J.: The 1200° C Cyclic Oxidation Behavior of Two Nickel-Aluminum Alloys ( $\text{Ni}_3\text{Al}$  and  $\text{NiAl}$ ) with additions of Chromium, Silicon, and Titanium. NASA TN D-6838, 1972.

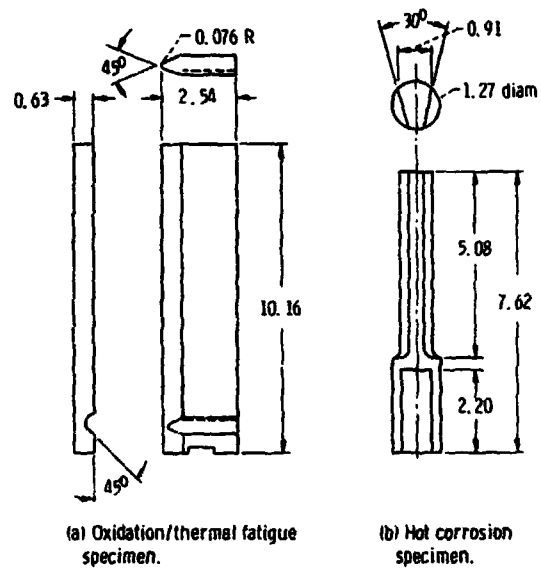
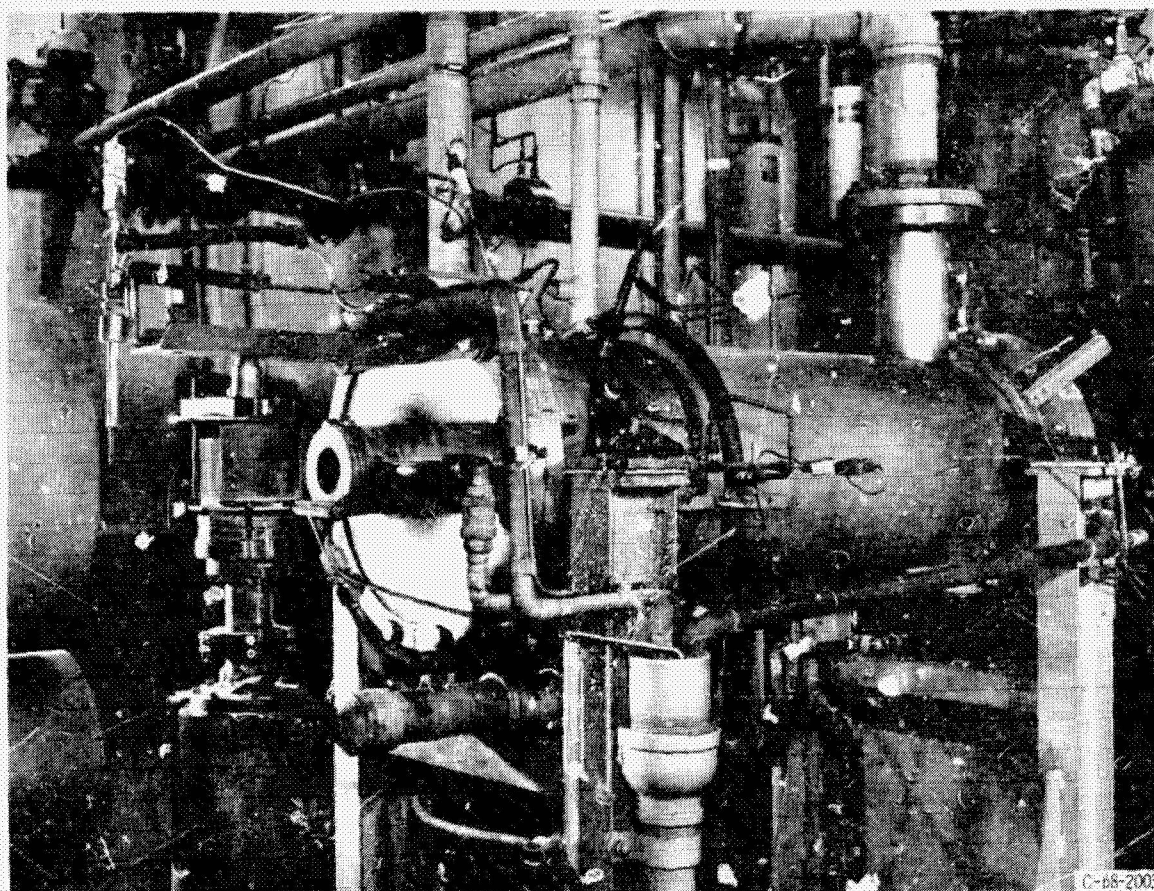
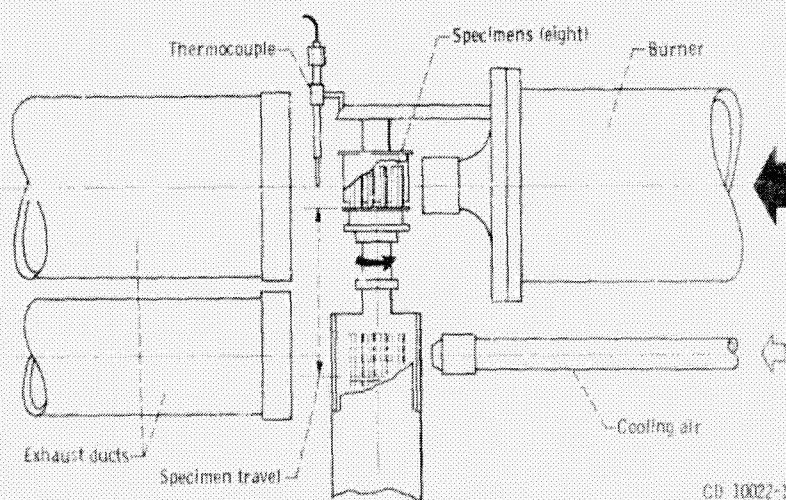


Figure 1. - High-gas-velocity test specimens. (Dimensions are in cm.)



C-68-2003

(a) Overall view.

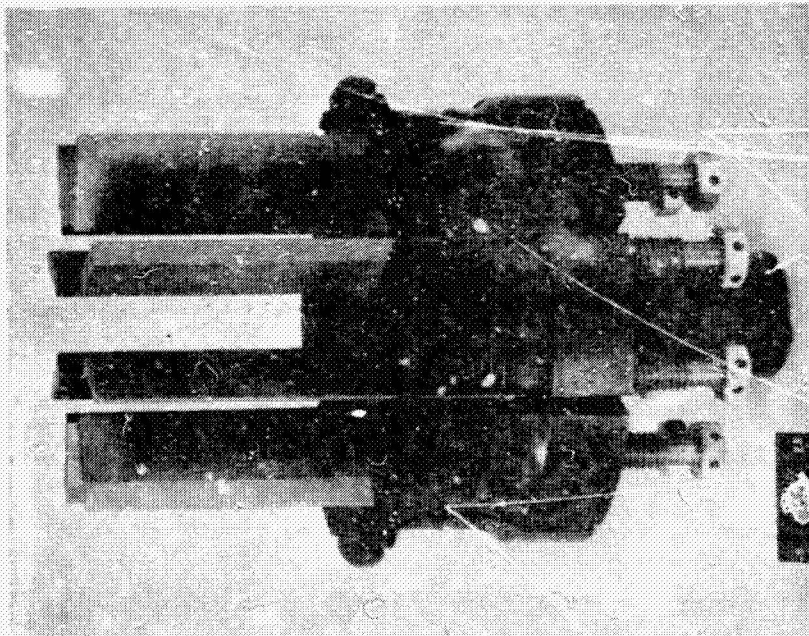


CD 10022-17

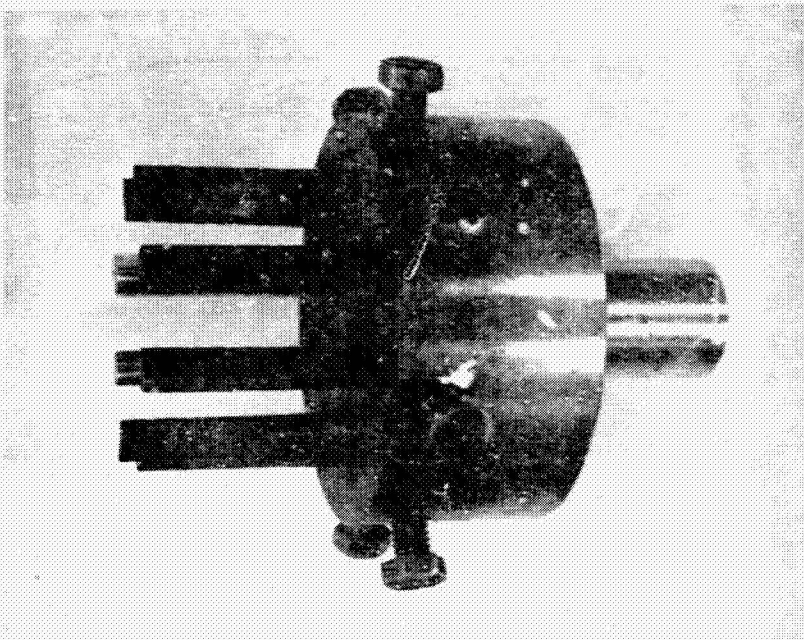
(b) Schematic diagram.

Figure 2. - High-gas-velocity oxidation apparatus.





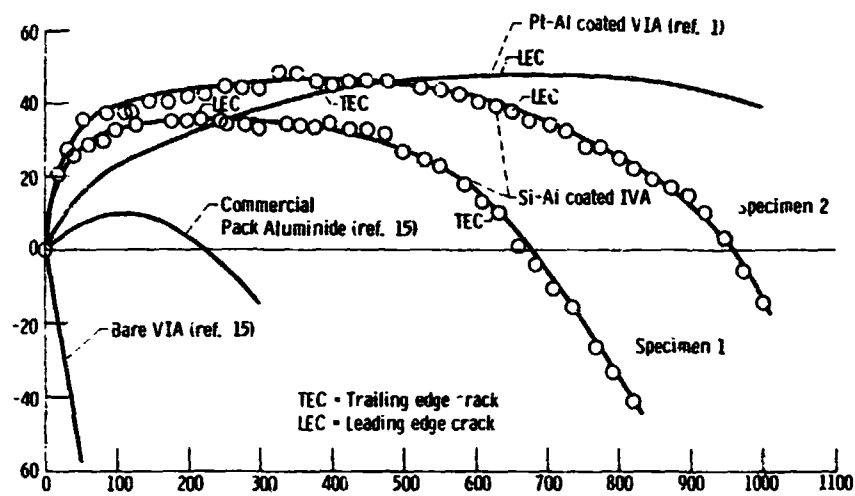
(a) Holder with oxidation specimens.



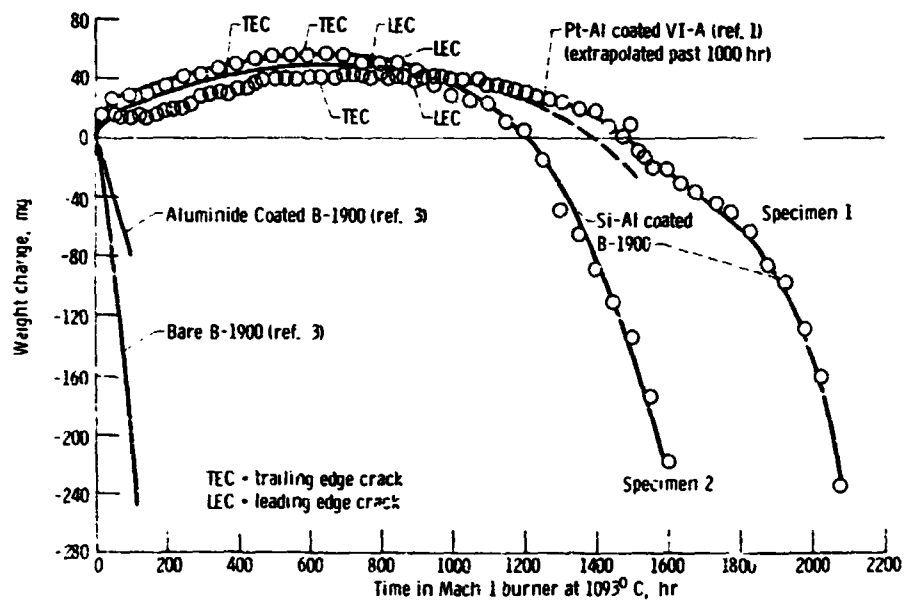
(b) Holder with hot-corrosion specimens.

Figure 3. - Specimen holder assemblies.

ORIGINAL PAGE IS  
OF POOR QUALITY



(a) Substrate alloy, VIA



(b) Substrate alloy, B-1900

Figure 4 - Comparison of bare and coated alloy response to high-gas-velocity (Mach 1) cyclic oxidation.

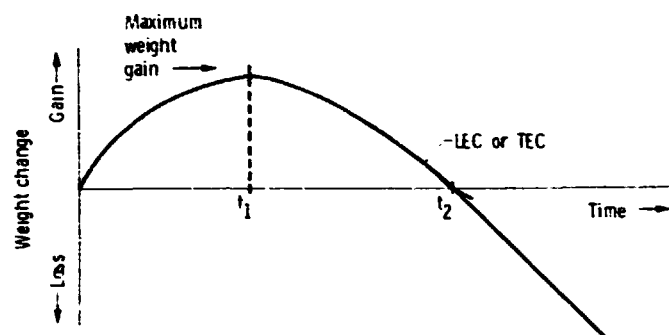
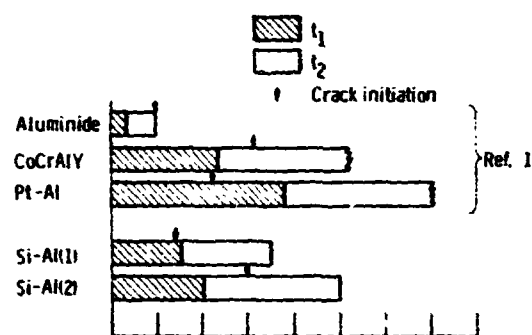
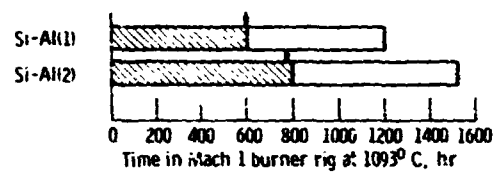


Figure 5. - Schematic diagram of weight-change curve for high-gas-velocity cyclic testing of coated superalloys. Time to maximum weight gain,  $t_1$ ; time at which curve crosses zero axis,  $t_2$ ; time at which first thermal fatigue crack is detected, LEC (for leading-edge crack) or TEC (for trailing-edge crack). (Ref. 1.)





(a) Substrate alloy, VIA.



(b) Substrate alloy, 9-1900.

Figure 6. - Comparison of oxidation parameters of Si-Al coating with those of reference 1.

ORIGINAL PAGE IS  
OF POOR QUALITY

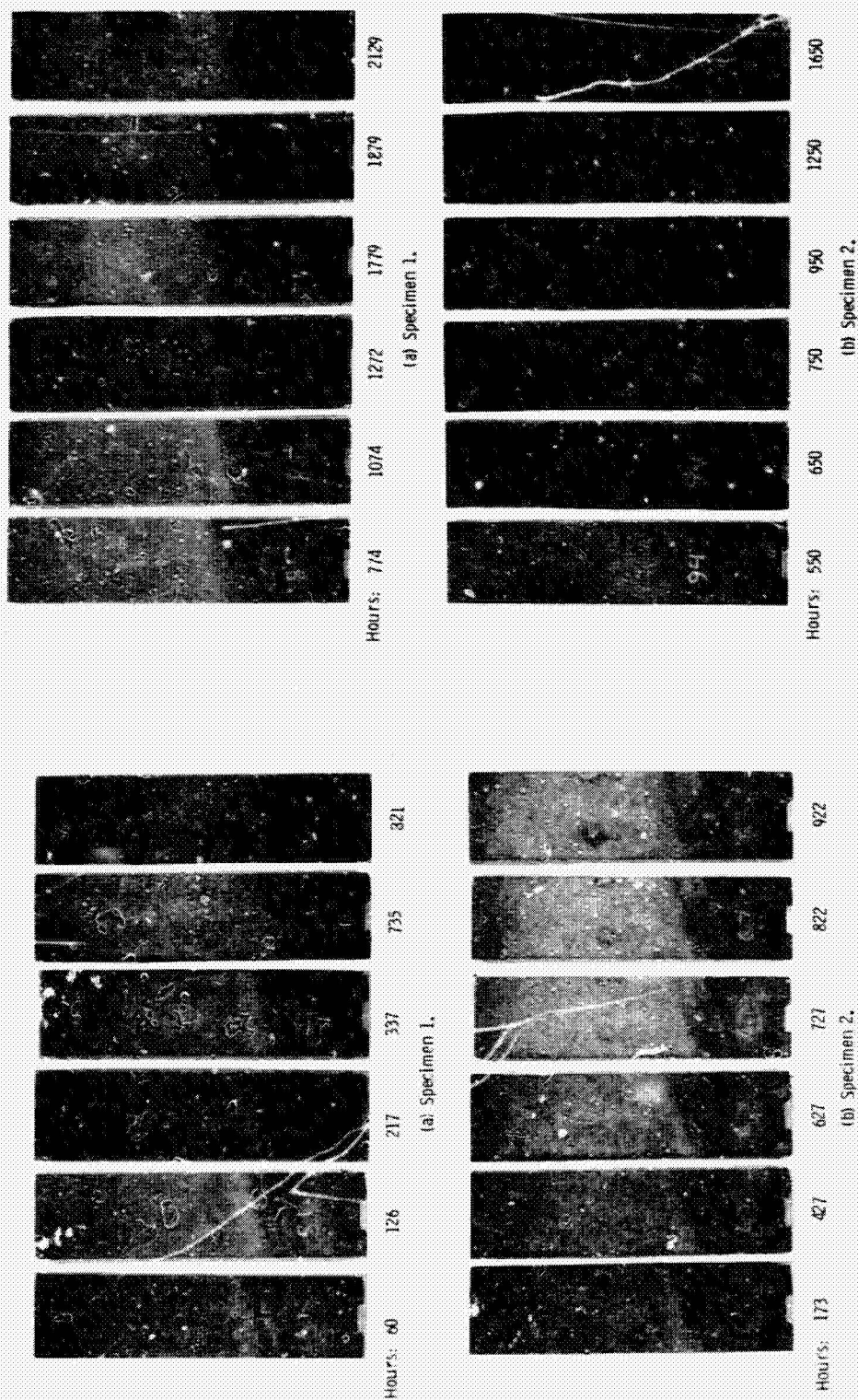


Figure 7. - Photomicrographs of Si-Al coated specimens of alloy V1A after Mach 1-gas-velocity cyclic oxidation at 1093°C for various numbers of 1-hour cycles.

Figure 8. - Photomicrographs of Si-Al coated specimens of B-1900 after Mach 1-gas-velocity cyclic oxidation at 1093°C for various numbers of 1-hour cycles.



Figure 9. - As-coated Si-Al on alloy VIA.

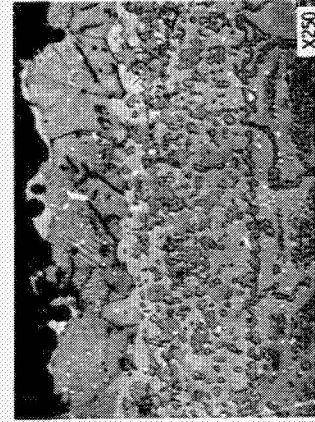
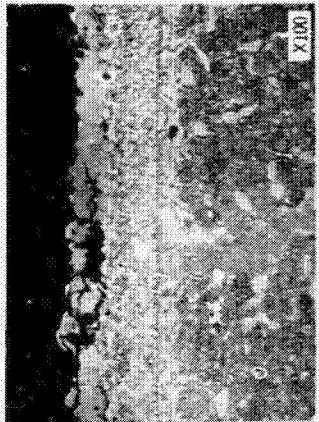


Figure 10. - Si-Al on alloy VIA after 1000, 1 hour cycles in Mach 1 burner at 1093°C, (view of tapered edge).

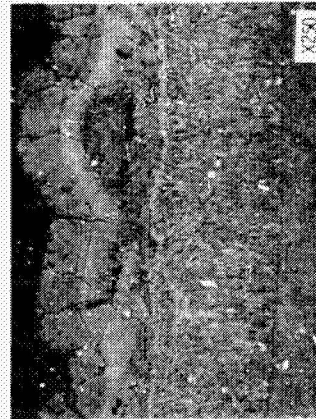
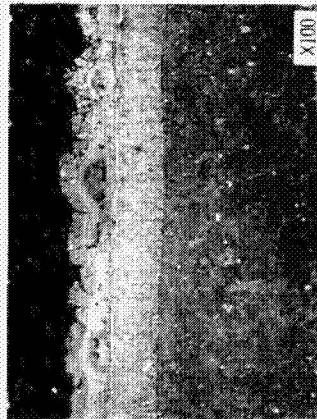


Figure 11. - As-coated Si-Al on alloy B-1900.

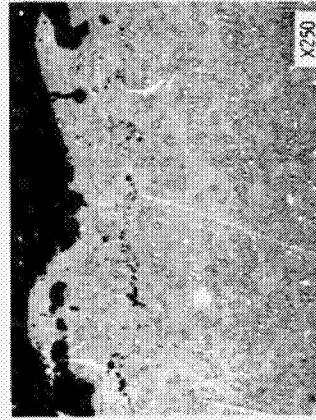
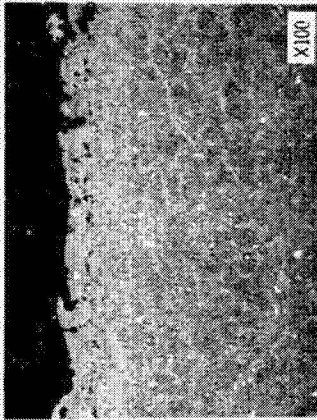


Figure 12. - Si-Al on alloy B-1900 after 2000, 1 hour oxidation cycles at 1093°C, (view of tapered edge).

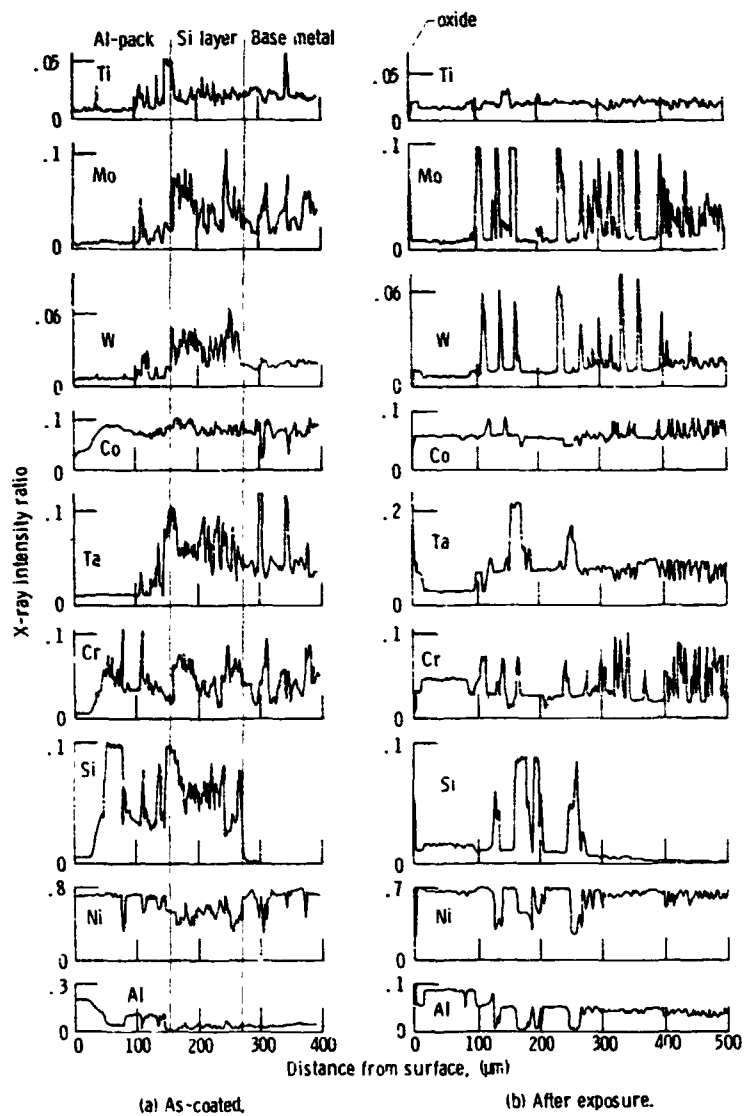


Figure 13 - Electron microprobe X-ray Analysis traces of oxidized, Si-Al surfaces into alloy VIA before and after 1000, 1-hr oxidation cycles at 1093° C.

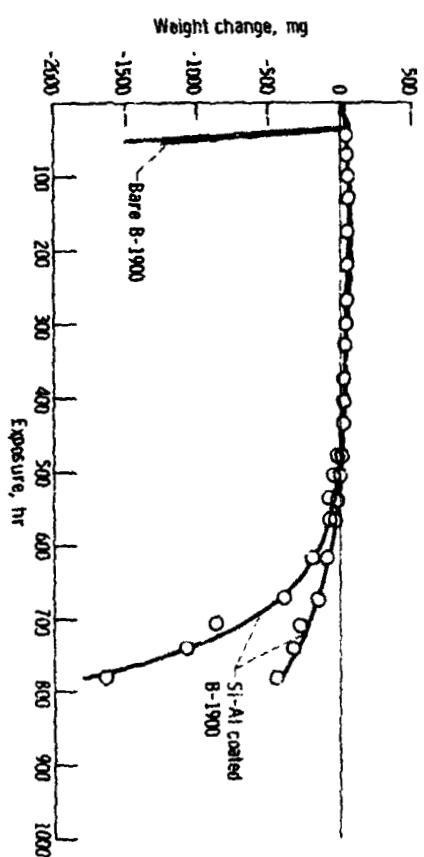


Figure 14. - Bare and coated B-1900 after Mach 0.3 hot-corrosion tests at 900° C for 1 hr in 5 ppm sea salt.



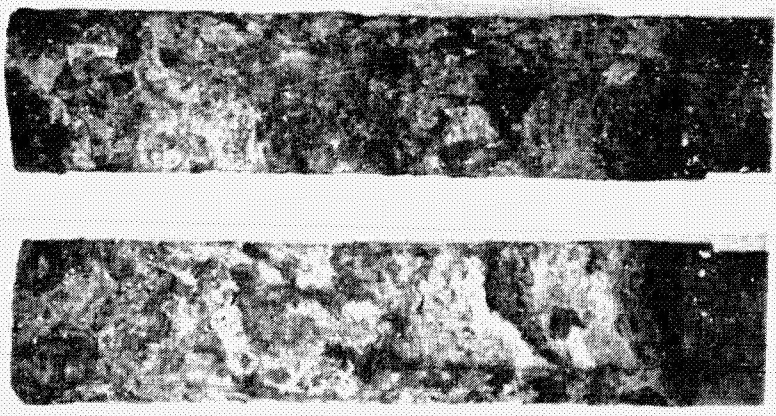
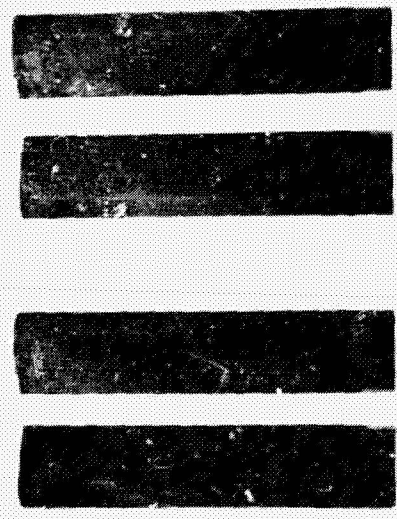


Figure 15. - Photomicrographs of uncoated B-1900 specimen after 105 Hrs of Mach 0.3 hot-corrosion tests at 900°C with 50ppm sea salt.



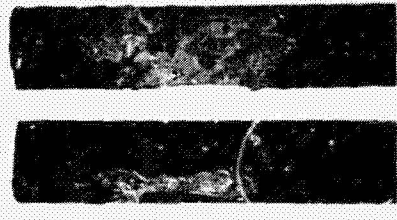
(a) Exposure, 238 Hrs.



(b) Exposure, 345 Hrs.



(c) Exposure, 638 Hrs.



(d) Exposure, 779 Hrs.

Figure 16. - Photomicrographs of Si-Al on B-1900 specimens after Mach 0.3 hot-corrosion tests at 900°C with sea salt.